Accurate WiFi Localization by Fusing a Group of Fingerprints via a Global Fusion Profile

Xiansheng Guo, *Member, IEEE*, Lin Li, *Student Member, IEEE*, Nirwan Ansari, *Fellow, IEEE*, and Bin Liao, *Senior Member, IEEE*

***Abstract*—The existing indoor localization approaches based on single fingerprints, such as received signal strength (RSS) and channel impulse response, are rather susceptible to the changing environment, multipath, and nonline-of-sight. It is well known that indoor localization can obtain higher positioning accuracy than the single-fingerprint-based methods by fusing multiple information sources (fingerprints/fingerprint functions). However, the existing fusion methods cannot fully exploit the intrinsic complementarity among multiple information sources and thus show lower accuracy. In this paper, we propose an accurate WiFi localization approach by Fusing A Group Of fingerprinTs (WiFi-FAGOT) via a global fusion profile (GFP). WiFi-FAGOT first constructs a WiFi-based GrOup Of Fingerprints (GOOF) in the offline phase, which consists of RSS, signal strength difference, and hyperbolic location fingerprint. Then, instead of direct localization by using the WiFi-based GOOF, we design multiple classifiers by training each fingerprint in the WiFi-based GOOF, namely GOOF classifiers. To fully leverage the intrinsic complementarity among different kinds of fingerprints, we propose a GFP construction algorithm by minimizing the average positioning error over the space of all GOOF classifiers. Finally, in the online phase, we derive a grid-dependent matching algorithm, namely, optimal classifier selection, to intelligently choose a fusion profile in the GFP for more accurate localization. Experimental results demonstrate that WiFi-FAGOT performs better than other systems in real complex indoor environments.**

***Index Terms*—WiFi, FAGOT, group of fingerprints (GOOF), global fusion profile (GFP), KNN.**

I. Introduction

The rapid growth of the Internet of Things (IoT) in which all kinds of physical devices and objects embedded with sensors are connected via a network of networks is spurring many emerging applications in various monitoring, control, transportation, and manufacturing systems [1], [2]. Many of these emerging applications require accurate localization, in particular, wireless indoor localization [3]–[6]. Although space-based satellite navigation systems such as global positioning system (GPS) offer high outdoor localization accuracy, the poor connectivity between satellites and end devices render them ineffective indoor, thus triggering further research on indoor localization [7]–[11] and navigation [12]–[14].

With the rapid development of wireless communications technology, there is an ever-increasing scope of WiFi applications, and almost each smartphone has a built-in WiFi module. Therefore, the WiFi-based indoor localization system has a broader range of applications than other techniques.

Existing WiFi-based localization algorithms mainly include geometric-based algorithms [15]–[18] and fingerprint-based algorithms [19], [20]. The former needs more accurate estimates of geometric parameters to yield a better location estimate. Nevertheless, the radio signal in a complex indoor environment is characterized by multipath fading, non-line-of-sight (NLOS) propagation and time-varying, and it is therefore unlikely to acquire the relative accurate geometric parameters, thus leading to cumulative localization errors. In contrast, the fingerprint-based approach does not need to estimate the geometric parameters and does not require the layout of the environment and the locations of the access points (AP), and has thus drawn much attention in recent years. However, the accuracy of the fingerprint-based approach is known to be vulnerable to an unpredictable changing environment.

To overcome the above drawbacks of the WiFi-based fingerprint system, several approaches have been proposed that can be categorized into constructing robust location features [21], [22], probabilistic methods [23], [24], and machine learning methods [25], [26]. These methods can improve the positioning accuracy to some extent, but they all employ single fingerprints, which are still not robust to a changing environment because a single fingerprint just captures the indoor environment from its own viewpoint/perspective.

It has been proven that information fusion is an efficient strategy to improve the drawbacks of the single fingerprints based localization approaches [27]–[31]. In [30], we first proposed a novel localization framework by fusing a group of fingerprints (FAGOT), which extracts different kinds of fingerprints in addition to the conventional RSS fingerprints from the received signals of multiple antennas to build a GrOup Of Fingerprints (GOOF). The fingerprints in GOOF describe an indoor environment from different perspectives, and so an efficient fusion of GOOF is expected to improve the localization performance significantly. Based on the constructed GOOF, we have derived

Manuscript received October 28, 2017; revised January 31, 2018 and April 2, 2018; accepted May 1, 2018. Date of publication May 3, 2018; date of current version August 13, 2018. This work was supported in part by the National Natural Science Foundation of China under Grant 61371184, Grant 61671137, Grant 61771114, and Grant 61771316, and in part by the Fundamental Research Funds for the Central Universities under Grant ZYGX2016J028. The review of this paper was coordinated by Prof. G. Mao. *(Corresponding author: Nirwan Ansari.)*

X. Guo and L. Li are with the Department of Electronic Engineering, University of Electronic Science and Technology of China, Chengdu 611731, China (e-mail: xsguo@uestc.edu.cn; linli9419@gmail.com).

N. Ansari is with the Advanced Networking Laboratory, Department of Electrical and Computer Engineering, New Jersey Institute of Technology, Newark, NJ 07102, USA (e-mail: nirwan.ansari@njit.edu).

B. Liao is with the College of Information Engineering, Shenzhen University, Shenzhen 518060, China (e-mail: binliao@szu.edu.cn).

Color versions of one or more of the figures in this paper are available online at http://ieeexplore.ieee.org.

Digital Object Identifier 10.1109/TVT.2018.2833029

a multiple classifiers multiple samples (MUCUS) fusion algorithm to obtain a more accurate location estimate.

In this paper, we propose an accurate WiFi localization approach by Fusing A Group Of fingerprinTs (WiFi-FAGOT) via global fusion profile (GFP). The key insight of our work is that each fingerprint can depict the localization environment from its particular perspective and can exhibit different advantages at different grid points. In the offline phase, WiFi-FAGOT first constructs a WiFi-based GOOF by extracting signal strength difference (SSD) and hyperbolic location fingerprint (HLF) from the RSS of WiFi signals. SSD and HLF pay more attention to pairwise information between APs, and thus are more robust to a changing environment and heterogeneous devices [21], [22]. Then, instead of direct localization by using the WiFi-based GOOF, we design multiple classifiers by training each fingerprint in the WiFi-based GOOF, namely, GOOF-classifiers. To fully leverage the intrinsic complementarity among different kinds of fingerprints, we propose a GFP construction algorithm by minimizing the average positioning error over the space of all GOOF-classifiers. Finally, in the online phase, we derive a grid-dependent matching algorithm, namely, optimal classifier selection (OCS), to intelligently select a fusion profile from GFP for more accurate localization. Experimental results show that our proposed system is superior to the existing methods in accuracy.

The contributions of this work are summarized below.

1) We propose a WiFi-based GOOF, which consists of RSS, SSD, and HLF. Although SSD and HLF are both derived from RSS, their combinations can improve the accuracy of localization significantly because SSD and HLF are more robust to a changing environment and heterogeneous devices.
2) We propose a more accurate WiFi-FAGOT localization framework by using the WiFi-based GOOF rather than the single RSS fingerprints. Instead of using the WiFi-based GOOF to localize target directly, WiFi-FAGOT first trains multiple GOOF-classifiers and fuse them efficiently for more accurate localization. The proposed framework does not require any hardware changes and is applicable to any WiFi-based systems.
3) We propose a GFP construction algorithm by minimizing the average positioning error over all GOOF-classifiers space with weights constraints in the offline phase. As compared with the existing fusion profile (FP) construction approaches, GFP can fully exploit the complementarity among different kinds of fingerprints, and thus yields a more accurate location estimate.
4) We propose an OCS matching algorithm to fully exploit the knowledge of the optimal classifier in the offline phase. OCS chooses the weights based on the output of the optimal classifier instead of RSS direct matching (RDM). It can overcome the impact of RSS fluctuation, and thus further improves the performance of localization.

The remaining paper is organized as follows. Section II introduces some works related to our study. The proposed WiFi-FAGOT framework, the WiFi-based GOOF construction, GOOF-classifiers training, GFP construction, OCS algorithm as well as performance analysis are represented in Section III. Section IV shows the experimental setup and results in real and simulation environments. Finally, conclusions are drawn in Section V. In addition, to improve readability, we summarize various acronyms used in this paper in Table I.

TABLE I
LIST OF ACRONYMS

Acronym	Definition
RSS	Received signal strength
SSD	Signal strength difference
HLF	Hyperbolic location fingerprint
GOOF	Group of fingerprints
FAGOT	Fusing a group of fingerprints
FP	Fusion profile
GFP	Global fusion profile
RDM	RSS direct matching
OCS	Optimal classifier selection
GDFP	Grid dependent fusion profile
GIFP	Grid independent fusion profile
DFC	Dynamic fingerprinting combining
MMSE	Minimum mean square error
DFPS	Delta-fused principle strength
MUCUS	Multiple classifiers multiple samples
PSD	Percentage standard deviation

II. Related Works

Fingerprint-based localization has attracted much attention recently because geometric-based algorithms show poor performance in complex indoor environments. In WiFi localization, RSS is one of the most attractive fingerprint due to the wide deployment and availability of WiFi infrastructures. However, the RSS-based localization system is not accurate and robust because RSS of WiFi is known to be vulnerable to unpredictable changing environments and hardware differences. To overcome the drawbacks of RSS, Kjrgaard *et al.* [22] proposed a hyperbolic location fingerprint (HLF) by recording fingerprints as signal strength ratios between pairs of base stations instead of absolute signal-strength values. HLF can solve the signal-strength difference problem without requiring extra manual calibration. Hossain *et al.* [21], [32] proposed a signal strength difference (SSD) fingerprint which outperforms the traditional RSS fingerprints in terms of robustness across heterogeneous mobile devices. In brief, HLF and SSD show small variations as compared with the RSS because they consider the pairwise information between APs. These fingerprints can improve the drawbacks of the RSS from different viewpoints. To combine the merits of these fingerprints, Fang *et al.* [33] proposed a delta-fused principle strength (DFPS) fingerprint which combines the delta signal strength (ΔRSS) with RSS to yield a more accurate localization result. A similar idea was adopted in [34]. The works in [33], [34] employ direct fusion of fingerprints. By different transformations of the received signals from a platform with multiple antennas, we first proposed a GOOF for more accurate localization [30]. The GOOF consists of five different fingerprints including RSS, covariance matrix, signal subspace, fourth-order cumulant, and fractional low-order moment; each fingerprint in the GOOF can depict the indoor environment from a unique perspective. Similar to [30], we propose a WiFi-based GOOF which includes RSS, SSD, and HLF for more accurate localization. The combination is done in the GOOF-classifiers space instead of the WiFi-based GOOF space, and is proven to further improve the accuracy of localization.

Fusion based localization has drawn much attention in recent years. The existing fusion methods can be categorized as two groups: one is the weighting fusion strategy [27]–[29], which trains fusion weights in the offline phase and uses these weights to fuse a better localization result in the online phase; the other is the direct fusion strategy in the online phase without using weights, such as multiple classifiers multiple samples (MUCUS) fusion method [30]. In general, the former shows better performance in accuracy improvement than the latter because it leverages the knowledge (weights) from the offline phase. The latter needs more online testing samples to yield one localization result, and is thus not very efficient because we cannot obtain more testing samples during the stationary phase of the target in a WiFi environment. Hence, the weighting fusion strategy is more practical than the direct fusion strategy in WiFi localization.

The existing weighting fusion strategies can be divided into two cases: one is based on a grid dependent fusion profile (GDFP), such as dynamic fingerprint combining (DFC) [27] and its variants [28], and the other is based on a grid independent fusion profile (GIFP), such as minimum mean square error (MMSE) based location estimation [29]. In a nutshell, the former constructs different fusion profiles at different grid points, while the latter trains one fusion profile for all grid points. Therefore, GDFP is superior to GIFP in a complex environment. However, the existing weighting strategies have two notable drawbacks: 1) The existing fusion profile (FP) is not globally optimal because it optimizes the weight for each classifier sequentially, and so they cannot make full use of the intrinsic complementarity among different kinds of fingerprints; 2) the weights selection method just uses a RSS direct matching strategy, which is very sensitive to RSS fluctuations, and thus leads to a large location error in a complex environment. Different from the above approaches, in this work, we propose a WiFi-based GOOF and derive a novel accurate WiFi localization by fusing the WiFi-based GOOF via a global fusion profile. Our proposed approach does improve the accuracy significantly as compared with the existing fusion methods.

III. Proposed Algorithm

A. WiFi-FAGOT Framework

Fig. 1 shows the functional blocks of our proposed WiFi-FAGOT framework, which consists of two phases: offline and online phase. Suppose that the location area can be divided into G grid points, each numbered by a label, and the area is covered by L WiFi APs. In the offline phase, we first construct the WiFi-based GOOF including RSS, SSD, and HLF. Assume that the WiFi-based GOOF can be divided into two groups, namely, $\boldsymbol{GF}$ and $\boldsymbol{GF}'$. Among them, $\boldsymbol{GF} = [\boldsymbol{D}_{RSS}, \boldsymbol{D}_{SSD}, \boldsymbol{D}_{HLF}]$ is used for GOOF-classifiers training, where $\boldsymbol{D}_{RSS}$, $\boldsymbol{D}_{SSD}$, and $\boldsymbol{D}_{HLF}$ denote the RSS, SSD and HLF fingerprints, respectively. Similarly, $\boldsymbol{GF}' = [\boldsymbol{D}'_{RSS}, \boldsymbol{D}'_{SSD}, \boldsymbol{D}'_{HLF}]$ is used for GFP construction and to find the optimal classifier, where $\boldsymbol{D}'_{RSS}$, $\boldsymbol{D}'_{SSD}$, and $\boldsymbol{D}'_{HLF}$ are also the corresponding RSS, SSD, and HLF fingerprints, respectively. These three kinds of fingerprints have their own advantages and disadvantages in dealing with changing environment and heterogeneous devices, and our proposed WiFi-FAGOT can exploit the complementarity among them to improve the positioning performance.

In the offline phase, we first train GOOF-classifiers by using the offline $\boldsymbol{GF}$ fingerprints. The classifier $f(\cdot)$ can be selected from either machine learning methods or probabilistic

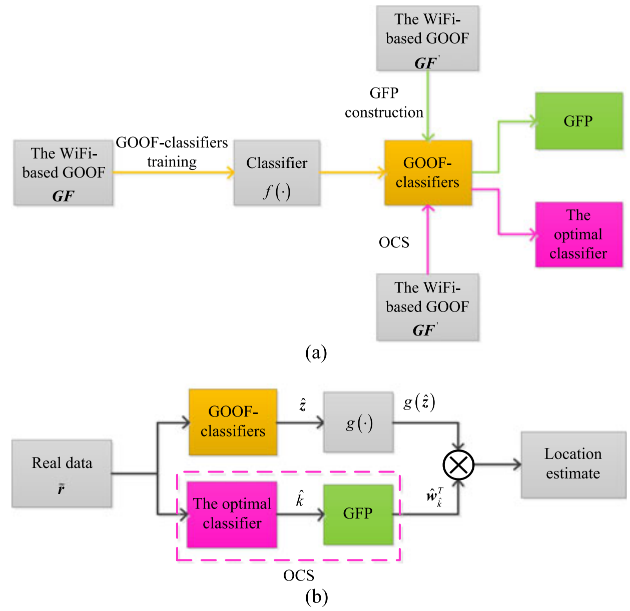

Fig. 1. The overview of our proposed WiFi-FAGOT framework. (a) Offline phase. (b) Online phase.

methods. Based on the GOOF-classifiers, we can further train GFP $\in \mathcal{R}^{3\times G}$ by using the offline fingerprints $\boldsymbol{GF}'$. GFP is a weighting matrix $\boldsymbol{W}$, which stores weights of different kinds of fingerprints at different grid points, and can be expressed as

$$\boldsymbol{W} = \begin{bmatrix} w_{11} & w_{21} & \cdots & w_{G1} \\ w_{12} & w_{22} & \cdots & w_{G2} \\ w_{13} & w_{23} & \cdots & w_{G3} \end{bmatrix} \tag{1}$$

in which the k-th column denotes the weights assigned for the GOOF-classifiers at the k-th grid point, i.e., the fusion profile of the k-th grid point. In addition, the optimal classifier needs to be chosen by the optimal classifier selection (OCS) with the same offline fingerprints $\boldsymbol{GF}'$, as shown in Fig. 1(a).

In the online phase, given a testing RSS sample, we can obtain multiple predictions $\hat{\boldsymbol{z}}$ from the trained GOOF-classifiers and the optimal weights selected by our proposed OCS algorithm. The final location estimate can be obtained by the inner product of the selected weights and the multiple predictions, as depicted in Fig. 1(b).

To clarify the implementation of our proposed WiFi-FAGOT, we give an example in Fig. 2. Considering an area with 25 grid points and the distance between two adjacent grid points is 0.5 m. Assume that GOOF-classifiers and GFP have already been constructed. Given a testing RSS sample with true grid point 13, we first transform it to SSD and HLF, respectively. Then, the predictions given by the GOOF-classifiers when inputting the testing samples of RSS, SSD and HLF are 9, 19 and 14, respectively, i.e., $\hat{z} = [9, 19, 14]^T$. These multiple predictions are then transformed into 2-D coordinates by the mapping function $g(\cdot)$, i.e.,

$$g(\hat{z}) = \begin{bmatrix} 0.5 & 0.5 \\ 0.5 & 1.5 \\ 1.5 & 1 \end{bmatrix}.$$

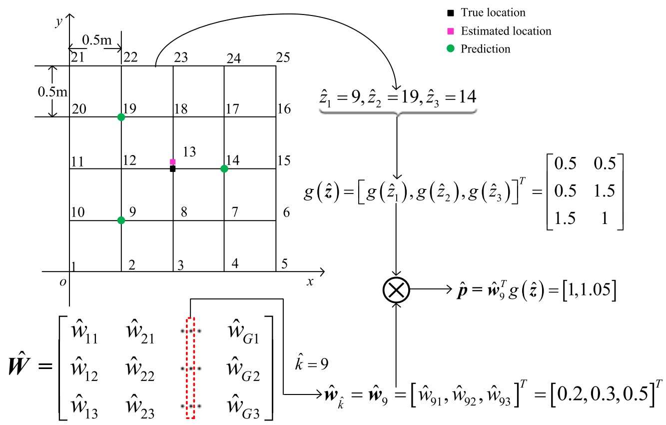

Fig. 2. An example of WiFi-FAGOT.

If the optimal classifier given in the offline phase is the one trained with $\boldsymbol{D}_{RSS}$, then the estimated grid point given by OCS should be 9, and so we can index the 9th column from the estimated GFP matrix $\hat{\boldsymbol{W}}$ and obtain the weights $\hat{\boldsymbol{w}}_9 = [0.2, 0.3, 0.5]^T$. The final estimated location is obtained by the inner product of the selected weights and the multiple predictions, i.e., the estimated location of target $\hat{\boldsymbol{p}} = \hat{\boldsymbol{w}}_9^T g(\hat{\boldsymbol{z}}) = [1, 1.05]$.

B. WiFi-Based GOOF

We first proposed GOOF in [30], which is constructed by transformations of the received signals of multiple antennas. However, the fingerprints extracted from the received signals of multiple antennas in [30] cannot be obtained by most commodity WiFi devices. So, we propose a WiFi-based GOOF, which can extract useful information from received WiFi signals. The WiFi-based GOOF includes three different kinds of fingerprints: RSS, SSD and HLF.

1) RSS: Denote $r_k^l(n)$ be the RSS value collected at the n-th time index, at the k-th grid point, and from the l-th AP. Denote $\boldsymbol{D}_{RSS}(k)$ as the M RSS samples collected at the k-th grid point:

$$\boldsymbol{D}_{RSS}(k) = [\boldsymbol{r}_k(1), \boldsymbol{r}_k(2), \ldots, \boldsymbol{r}_k(M)] = \begin{bmatrix} r_k^1(1) & r_k^1(2) & \cdots & r_k^1(M) \\ r_k^2(1) & r_k^2(2) & \cdots & r_k^2(M) \\ \vdots & \vdots & \ddots & \vdots \\ r_k^L(1) & r_k^L(2) & \cdots & r_k^L(M) \end{bmatrix}, \quad (2)$$

in which M is the number of the collected RSS samples for training classifiers and $\boldsymbol{r}_k(m) = [r_k^1(m), r_k^2(m), \ldots, r_k^L(m)]^T$, $(m = 1, 2, \ldots, M, k = 1, 2, \ldots, G)$. Then, the RSS fingerprints for GOOF-classifiers training at all grid points can be expressed as $\boldsymbol{D}_{RSS} = [\boldsymbol{D}_{RSS}(1), \boldsymbol{D}_{RSS}(2), \ldots, \boldsymbol{D}_{RSS}(G)] \in \mathcal{R}^{L\times M\times G}$.

Similarly, denote $\boldsymbol{D}'_{RSS}(k)$ as N RSS samples collected at the k-th grid point:

$$\boldsymbol{D}'_{RSS}(k) = [\boldsymbol{r}_k(M+1), \boldsymbol{r}_k(M+2), \ldots, \boldsymbol{r}_k(M+N)] \quad (3)$$

where $\boldsymbol{r}_k(n) = [r_k^1(n), r_k^2(n), \ldots, r_k^L(n)]^T, (n = M+1, M+2, \ldots, M+N)$. So, the fingerprints for GFP construction and the optimal classifier selection at all grid points can be expressed as $\boldsymbol{D}'_{RSS} = [\boldsymbol{D}'_{RSS}(1), \boldsymbol{D}'_{RSS}(2), \ldots, \boldsymbol{D}'_{RSS}(G)] \in \mathcal{R}^{L\times N\times G}$.

2) SSD: SSD calculates the differences of the RSS values between pairs of APs to construct a new robust position feature [21]. The primary goal of SSD is to eliminate the variation caused by heterogeneous devices. It is calculated as

$$\Delta r_k^{ij}(n) = r_k^i(m) - r_k^j(m), i \in [1, L-1], j \in [2, L], i < j \quad (4)$$

According to (4), the submatrix $\boldsymbol{D}_{SSD}(k)$ can be written as

$$\boldsymbol{D}_{SSD}(k) = [\Delta\boldsymbol{r}_k(1), \Delta\boldsymbol{r}_k(2), \ldots, \Delta\boldsymbol{r}_k(M)] \quad (5)$$

with $\Delta\boldsymbol{r}_k(m) = [\Delta r_k^{12}(m), \Delta r_k^{13}(m), \ldots, \Delta r_k^{(L-1)L}(m)]^T$, $(m = 1, 2, \ldots, M)$. Similarly, we can obtain $\boldsymbol{D}'_{SSD}(k)$ as

$$\boldsymbol{D}'_{SSD}(k) = [\Delta\boldsymbol{r}_k(M+1), \ldots, \Delta\boldsymbol{r}_k(M+N)] \quad (6)$$

with $\Delta\boldsymbol{r}_k(n) = [\Delta r_k^{12}(n), \Delta r_k^{13}(n), \ldots, \Delta r_k^{(L-1)L}(n)]^T, (n = M+1, M+2, \ldots, M+N)$. SSD can reduce the effect of the variation of RSS because it has smaller variance as compared with RSS.

3) HLF: HLF [22] has also been proposed to mitigate the hardware heterogeneity problem, and it uses ratios of the RSSs between pairs of APs as fingerprints; it first converts RSS from dBm to numerical values between 0 and 255. Denote $\gamma_k^l(n)$ as the converted value of $r_k^l(n)$, which can be express as

$$\gamma_k^l(n) = 255 + r_k^l(n). \quad (7)$$

The normalized logarithm signal strength ratio $\eta_k^{ij}(n)$ between the i-th and j-th AP at the k-th grid point can be calculated as

$$\eta_k^{ij}(n) = \log\left(\frac{\gamma_k^i(n)}{\gamma_k^j(n)}\right) - \log\left(\frac{1}{\gamma_{\max}}\right) \quad (8)$$

where $\gamma_{\max} = \max\{\gamma_k^1(n), \gamma_k^2(n), \ldots, \gamma_k^L(n)\}$. The ranges of i and j are the same as those of (4). According to (8), the submatrix $\boldsymbol{D}_{HLF}(k)$ can be written as

$$\boldsymbol{D}_{HLF}(k) = [\boldsymbol{\eta}_k(1), \boldsymbol{\eta}_k(2), \ldots, \boldsymbol{\eta}_k(M)] \quad (9)$$

where $\boldsymbol{\eta}_k(m) = [\eta_k^{12}(m), \eta_k^{13}(m) \ldots, \eta_k^{(L-1)L}(m)]^T$, $(m = 1, 2, \ldots, M)$. Similarly, we can obtain $\boldsymbol{D}'_{HLF}$ as

$$\boldsymbol{D}'_{HLF}(k) = [\boldsymbol{\eta}_k(M+1), \ldots, \boldsymbol{\eta}_k(M+N)] \quad (10)$$

where $\boldsymbol{\eta}_k(n) = [\eta_k^{12}(n), \eta_k^{13}(n) \ldots, \eta_k^{(L-1)L}(n)]^T$, $(n = M+1, M+2, \ldots, M+N)$. As compared with SSD, HLF shows smaller variance and is more robust to a changing environment.

Then, we can construct our proposed WiFi-based GOOF for GOOF-classifiers training as $\boldsymbol{GF} = [\boldsymbol{D}_{RSS}, \boldsymbol{D}_{SSD}, \boldsymbol{D}_{HLF}]$. Similarly, the WiFi-based GOOF for GFP training and the optimal classifier selection can be written as $\boldsymbol{GF}' = [\boldsymbol{D}'_{RSS}, \boldsymbol{D}'_{SSD}, \boldsymbol{D}'_{HLF}]$. For simplicity, we number the set of fingerprints in the WiFi-based GOOF as $\boldsymbol{GF}_1 = \boldsymbol{D}_{RSS}$, $\boldsymbol{GF}_2 = \boldsymbol{D}_{SSD}$, and $\boldsymbol{GF}_3 = \boldsymbol{D}_{HLF}$, respectively. Similarly, we have $\boldsymbol{GF}'_1 = \boldsymbol{D}'_{RSS}$, $\boldsymbol{GF}'_2 = \boldsymbol{D}'_{SSD}$, and $\boldsymbol{GF}'_3 = \boldsymbol{D}'_{HLF}$.

C. GOOF-Classifier Training

Specifically, the classifier refers to a function that maps an input vector to a corresponding label (i.e., grid position/location).

The classifier should be trained first with offline fingerprints to learn a general rule by mapping inputs to outputs. Then, the classifier can make predictions based on the unseen online RSS measurements.

Let $f(\cdot)$ be a classifier trained with $\boldsymbol{GF}$ that maps a training vector to a corresponding label (i.e., grid position/location). $f(\cdot)$ mainly falls into two categories: machine learning and probabilistic models. Machine learning models include k-nearest neighbors (KNN), support vector machine (SVM) and random forest (RF) (to mention just a few) [25], [26]. Probabilistic models include Bayesian classifier, expectation maximization, Gaussian process, etc. [23], [24]. We then train GOOF-classifiers $f(\boldsymbol{GF}_1)$, $f(\boldsymbol{GF}_2)$, and $f(\boldsymbol{GF}_3)$ by using three different kinds of fingerprints in the WiFi-based GOOF, i.e., $\boldsymbol{GF}_1$, $\boldsymbol{GF}_2$, and $\boldsymbol{GF}_3$.

In this paper, we select KNN as our basis classifier, which is a type of instance-based learning, or lazy learning. It is the simplest one among all machine learning algorithms [35]. KNN calculates the distance between an online testing vector and each vector in the trained data by using a given distance metric. Here, we use the Euclidean distance to determine the location.

D. GFP Construction

In the offline phase, we can obtain the predictions based on the above trained classifiers by inputting the offline GFP training data ($\boldsymbol{GF}'$), i.e., $\boldsymbol{GF}'_1$, $\boldsymbol{GF}'_2$, and $\boldsymbol{GF}'_3$. At the k-th grid point, we have

$$\begin{cases} \hat{z}_1^k(n) = f(\boldsymbol{r}_k(n), \boldsymbol{GF}_1) \\ \hat{z}_2^k(n) = f(\Delta\boldsymbol{r}_k(n), \boldsymbol{GF}_2) \\ \hat{z}_3^k(n) = f(\boldsymbol{\eta}_k(n), \boldsymbol{GF}_3), \end{cases} \tag{11}$$

where $\hat{z}_h^k(n)\,(h = 1, 2, 3, n = M+1, \ldots, M+N)$ is the prediction of the corresponding sample of the h-th fingerprint, $\boldsymbol{r}_k(n) \in \boldsymbol{GF}'_1$, $\Delta\boldsymbol{r}_k(n) \in \boldsymbol{GF}'_2$, and $\boldsymbol{\eta}_k(n) \in \boldsymbol{GF}'_3$.

The existing fusion profile (FP) construction was proposed in DFC [27], which searches for the weights sequentially by minimizing the average positioning error over N samples. By exploring this strategy, the weights of RSS, SSD, and HLF are sequentially estimated as

$$\hat{w}_{k1} = \mathop{\arg\min}_{0\le w_{k1}\le 1} \frac{1}{N}\sum_{n=M+1}^{N+M} e\left(\boldsymbol{r}_k(n)\middle|\, w_{k1}\right), \tag{12}$$

$$\hat{w}_{k2} = \mathop{\arg\min}_{0\le w_{k2}\le 1} \frac{1}{N}\sum_{n=M+1}^{N+M} e\left(\Delta\boldsymbol{r}_k(n)\middle|\, w_{k2}\right), \tag{13}$$

$$\hat{w}_{k3} = \mathop{\arg\min}_{0\le w_{k3}\le 1} \frac{1}{N}\sum_{n=M+1}^{N+M} e\left(\boldsymbol{\eta}_k(n)\middle|\, w_{k3}\right), \tag{14}$$

where $e(\boldsymbol{r}_k(n)|\, w_{k1})$, $e(\Delta\boldsymbol{r}_k(n)|\, w_{k2})$, and $e(\boldsymbol{\eta}_k(n)|\, w_{k3})$ are the localization errors for the n-th RSS, SSD, and HLF samples at the k-th grid point with the weights w_{k1}, w_{k2}, and w_{k3}, respectively, that is,

$$e\left(\boldsymbol{r}_k(n)\middle|\, w_{k1}\right) = \left\| w_{k1} \times g\left(\hat{z}_1^k(n)\right) - \boldsymbol{p}_k \right\|_2, \tag{15}$$

$$e\left(\Delta\boldsymbol{r}_k(n)\middle|\, w_{k2}\right) = \left\| w_{k2} \times g\left(\hat{z}_2^k(n)\right) - \boldsymbol{p}_k \right\|_2, \tag{16}$$

$$e\left(\boldsymbol{\eta}_k(n)\middle|\, w_{k3}\right) = \left\| w_{k3} \times g\left(\hat{z}_3^k(n)\right) - \boldsymbol{p}_k \right\|_2, \tag{17}$$

where $\|\cdot\|_2$ is the ℓ_2-norm and $\boldsymbol{p}_k = [x_k, y_k]^T$ is the known location of the k-th grid point. $\hat{z}_1^k(n)$, $\hat{z}_2^k(n)$, and $\hat{z}_3^k(n)$ are given by (11). $g(\cdot) : \mathcal{R}^1 \to \mathcal{R}^2$ maps a label (i.e., grid position/location) to a 2-D coordinate.

After having obtained all the weights of multiple classifiers sequentially, they are normalized together according to

$$\sum_{h=1}^{3} \hat{w}_{kh} = 1, k = 1, 2, \ldots, G. \tag{18}$$

Note that the weights searching strategy by using (12)–(18) is just the optimization for each classifier over all N samples. It cannot fully excavate the intrinsic complementarity among different kinds of fingerprints. Therefore, the FP of DFC is not a global optimal solution.

To overcome the drawback of FP, we propose a GFP construction algorithm as follows. Let $\boldsymbol{w}_k = [w_{k1}, w_{k2}, w_{k3}]^T$ be the k-th weight vector in the GFP, which can be constructed by minimizing the average positioning error over all GOOF-classifiers space as follows

$$\begin{aligned} \hat{\boldsymbol{w}}_k = \min_{\boldsymbol{w}_k} \frac{1}{N} &\sum_{n=M+1}^{N+M} e'\left(\hat{\boldsymbol{z}}^k(n)|\boldsymbol{w}_k\right) \\ \text{s.t. } &\boldsymbol{w}_k^T\mathbf{1} = 1, \\ &w_{kh} \ge 0, h = 1, 2, 3 \end{aligned} \tag{19}$$

where $\mathbf{1}$ is a 3×1 all one vector. The localization error $e'(\hat{\boldsymbol{z}}^k(n)|\boldsymbol{w}_k)$ is given by

$$e'\left(\hat{\boldsymbol{z}}^k(n)|\boldsymbol{w}_k\right) = \left\|\boldsymbol{w}_k^T g\left(\hat{\boldsymbol{z}}^k(n)\right) - \boldsymbol{p}_k\right\|_2, \tag{20}$$

where $\hat{\boldsymbol{z}}^k(n) = [\hat{z}_1^k(n), \hat{z}_2^k(n), \hat{z}_3^k(n)]^T$ with $\hat{z}_h^k(n)$ being given by (11). Equation (19) is a nonlinear optimization problem; in this work, we solve it by quasi-Newton method, which achieves rapid convergence.

After having obtained $\hat{\boldsymbol{w}}_k$, the estimated GFP matrix can be given by

$$\hat{\boldsymbol{W}} = [\hat{\boldsymbol{w}}_1, \hat{\boldsymbol{w}}_2, \ldots, \hat{\boldsymbol{w}}_G]. \tag{21}$$

Our proposed GFP can be obtained by solving the optimization problem depicted in (19) and (20), which is a joint optimization of multiple classifiers. As compared with the FP constructed from DFC, our proposed GFP can excavate the complementarity among different kinds of fingerprints. We summarize the procedure of constructing GFP in Algorithm 1.

E. Optimal Classifier Selection (OCS)

After having obtained GFP, another key problem for accurate fusion localization is to choose the optimal weights for fusing the outputs of the trained classifiers when given an RSS testing sample $\tilde{\boldsymbol{r}}$ in the online phase, i.e., how to estimate a suitable grid index $\hat{k}$ for $\tilde{\boldsymbol{r}}$? The existing $\hat{k}$ estimation method is RDM between the testing sample $\tilde{\boldsymbol{r}}$ and the training fingerprints $\boldsymbol{GF}_1$, that is

$$\hat{k} = \mathop{\arg\min}_{k} \left\|\tilde{\boldsymbol{r}} - \overline{\boldsymbol{GF}}_1(k)\right\|_2 \tag{22}$$

where $\overline{\boldsymbol{GF}}_1(k)$ is the mean vector of the $\boldsymbol{GF}_1(k)$. However, this matching strategy is easily affected by the fluctuation of RSS

Algorithm 1: GFP construction.

Input: 1) The number of grid points G; 2) The WiFi-based GOOF for GFP construction $\boldsymbol{GF}'$; 3)The trained GOOF-classifiers, i.e., $f(\boldsymbol{GF}_1)$, $f(\boldsymbol{GF}_2)$, and $f(\boldsymbol{GF}_3)$;

Output: The estimate of GFP matrix $\hat{\boldsymbol{W}}$

1: **for** $k = \{1, 2, \ldots, G\}$ **do**
2:   **for** $n = \{M+1, M+2, \ldots, M+N\}$ **do**
3:     Compute prediction vector $\hat{z}_1^k(n)$, $\hat{z}_2^k(n)$, and $\hat{z}_3^k(n)$ by using (11)
4:     Compute the positioning error by using (20)
5:   **end for**
6:   Compute the k-th weight vector by using (19)
7: **end for**
8: $\hat{\boldsymbol{W}} = [\hat{\boldsymbol{w}}_1, \hat{\boldsymbol{w}}_2, \ldots, \hat{\boldsymbol{w}}_G]$
9: **return** $\hat{\boldsymbol{W}}$

in complex indoor environments, and leads to an additional matching error to the localization system.

To overcome this drawback, we propose an OCS algorithm. Firstly, we find the optimal classifier in the offline phase by minimizing the positioning errors as follows

$$\hat{h} = \arg\min_{h} \sum_{k=1}^{G} \sum_{n=M+1}^{N+M} \left\| g\left(\hat{z}_h^k(n)\right) - \boldsymbol{p}_k \right\|_2, \tag{23}$$

where $\hat{z}_h^k(n)$ is the prediction of the h-th classifier, as shown in (11).

In the online phase, assume that we receive a testing RSS sample $\tilde{\boldsymbol{r}}$, we then transform it into SSD $\Delta\tilde{\boldsymbol{r}}$ and HLF $\tilde{\boldsymbol{\eta}}$. For simplicity, we let $\tilde{\boldsymbol{\theta}}_1 = \tilde{\boldsymbol{r}}$, $\tilde{\boldsymbol{\theta}}_2 = \Delta\tilde{\boldsymbol{r}}$ and $\tilde{\boldsymbol{\theta}}_3 = \tilde{\boldsymbol{\eta}}$. Given the index of the optimal classifier $\hat{h}$, we can obtain $\tilde{\boldsymbol{\theta}}_{\hat{h}}$. Then, the matching grid point can be given as

$$\hat{k} = f\left(\tilde{\boldsymbol{\theta}}_{\hat{h}}, \boldsymbol{GF}_{\hat{h}}\right), \tag{24}$$

Then, the optimal weights $\hat{\boldsymbol{w}}_{\hat{k}}$ will be selected from the estimated GFP matrix $\hat{\boldsymbol{W}}$ based on the estimated grid point $\hat{k}$. Equations (23) and (24) are the main steps of our proposed OCS algorithm, as summarized in Algorithm 2. OCS could choose the weights based on the output of the optimal classifier; in other words, it selects the optimal weights by resorting to the knowledge of the optimal classifier. So, it is superior to the RDM method adopted by DFC.

Given the matching grid point obtained by the OCS algorithm, the final location estimate is given by

$$\hat{\boldsymbol{p}} = \hat{\boldsymbol{w}}_{\hat{k}}^T g\left(\hat{\boldsymbol{z}}\right), \tag{25}$$

where $\hat{\boldsymbol{z}} = [f(\tilde{\boldsymbol{\theta}}_1, \boldsymbol{GF}_1), f(\tilde{\boldsymbol{\theta}}_2, \boldsymbol{GF}_2), f(\tilde{\boldsymbol{\theta}}_3, \boldsymbol{GF}_3)]^T$.

F. Performance Analysis

1) Robustness: The three fingerprints, RSS, SSD, and HLF in the WiFi-based GOOF show different intrinsic characteristics. Although both SSD and HLF can reduce the impact of heterogeneous devices, they adopt different strategies. SSD calculates the differences of the RSS values between pairs of APs, while HLF uses ratios of the RSS values between pairs of APs and then normalizes the ratios. To show the intrinsic characteristics of the three fingerprints, we define two metrics, namely, the percentage of standard deviation (PSD) σ and correlation coefficient ρ. The PSDs of RSS, SSD and HLF can be expressed as

$$\begin{cases} \sigma_{k,\mathrm{RSS}}^{l} = \frac{\sqrt{\frac{1}{M}\sum_{m=1}^{M}\left[r_k^l(m) - \mu_r\right]^2}}{|\mu_r|} \times \% \\ \sigma_{k,\mathrm{SSD}}^{ij} = \frac{\sqrt{\frac{1}{M}\sum_{m=1}^{M}\left[\Delta r_k^{ij}(m) - \mu_{\Delta r}\right]^2}}{|\mu_{\Delta r}|} \times \% \\ \sigma_{k,\mathrm{HLF}}^{ij} = \frac{\sqrt{\frac{1}{M}\sum_{m=1}^{M}\left[\eta_k^{ij}(m) - \mu_\eta\right]^2}}{|\mu_\eta|} \times \% \end{cases} \tag{26}$$

where μ_r, $\mu_{\Delta r}$, and μ_η are the mean values of $\boldsymbol{D}_{RSS}(k)$, $\boldsymbol{D}_{SSD}(k)$, and $\boldsymbol{D}_{HLF}(k)$, respectively; $|\cdot|$ denotes the absolute value. Note that PSD is a metric to evaluate the ability of a fingerprint against a changing environment because it is a statistic on different time index m. The smaller the PSD, the more robust the fingerprint.

The correlation coefficient $\rho(j)$ between the fingerprint vectors at the k-th and the $(k+j)$-th grid points is given

$$\begin{cases} \rho_{\mathrm{RSS}}(j) = \frac{\boldsymbol{r}_k^T \boldsymbol{r}_{k+j}}{\|\boldsymbol{r}_k\|_2 \|\boldsymbol{r}_{k+j}\|_2} \\ \rho_{\mathrm{SSD}}(j) = \frac{\Delta\boldsymbol{r}_k^T \Delta\boldsymbol{r}_{k+j}}{\|\Delta\boldsymbol{r}_k\|_2 \|\boldsymbol{r}_{k+j}\|_2} \\ \rho_{\mathrm{HLF}}(j) = \frac{\boldsymbol{\eta}_k^T \boldsymbol{\eta}_{k+j}}{\|\boldsymbol{\eta}_k\|_2 \left\|\boldsymbol{\eta}_{k+j}\right\|_2}. \end{cases} \tag{27}$$

Note that the correlation coefficient reflects the spatial discrimination among grid points, the bigger ρ, the poorer spatial discrimination.

Here, we conducted a small experiment with two different smartphones (Vivo and Huawei). We collected 100 RSS samples at each grid point for both devices. Then, we calculated the mean RSS measurement at each grid point. Fig. 3(a) shows the mean RSS measurements at the 1st AP. The mean PSD of RSS of two devices is 14.9% as shown in Table II. Fig. 3(b) and (c) show the SSD and HLF values between the 1st and 2nd APs. The PSDs of SSD and HLF are 7.1% and 3.6%, respectively, which demonstrate that SSD and HLF can reduce the variation caused by heterogeneous devices and are more robust to changing environments.

With respect to spatial discrimination, Table II lists the mean correlation coefficients among different grid points. We find that SSD and HLF yield bigger ρ than RSS does. The correlation coefficients of SSD and HLF are 0.6302 and 0.8276, respectively. That is, SSD and HLF show poorer spatial discrimination as compared with RSS.

In summary, RSS, SSD, and HLF have their own advantages and disadvantages in dealing with heterogeneous devices,

Algorithm 2: OCS.

Input: 1) The testing sample $\tilde{\boldsymbol{r}}$; 2) The trained GOOF-classifiers, i.e., $f(\boldsymbol{D}_{RSS})$, $f(\boldsymbol{D}_{SSD})$, and $f(\boldsymbol{D}_{HLF})$; 3) The index of the optimal classifier $\hat{h}$;

Output: The estimated grid point $\hat{k}$

1: Transform $\Delta\tilde{\boldsymbol{r}}$ and $\tilde{\boldsymbol{\eta}}$ from $\tilde{\boldsymbol{r}}$
2: Find $\tilde{\boldsymbol{\theta}}_{\hat{h}}$ by using $\hat{h}$
3: Compute the grid point estimate $\hat{k}$ by using (24)
4: **return** $\hat{k}$

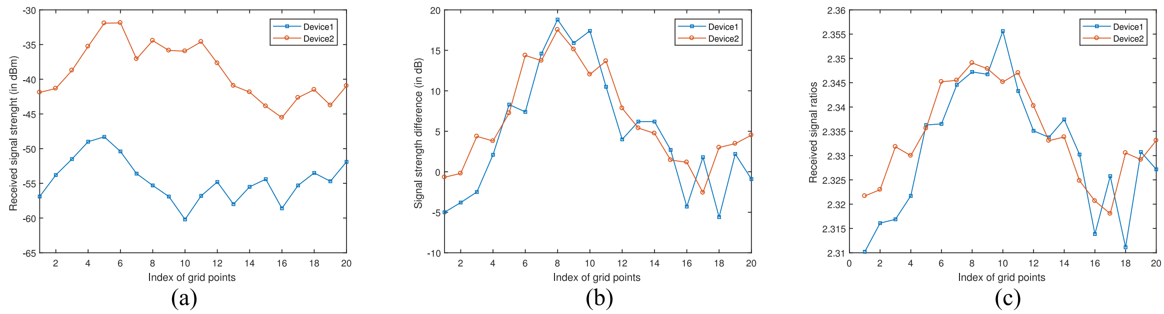

Fig. 3. The RSS, SSD, and HLF values considering heterogeneous devices at different grid points. (a) The mean RSS measurements collected at the 1st AP. (b) The SSD values between the 1st and 2nd APs. (c) The HLF values between the 1st and 2nd APs.

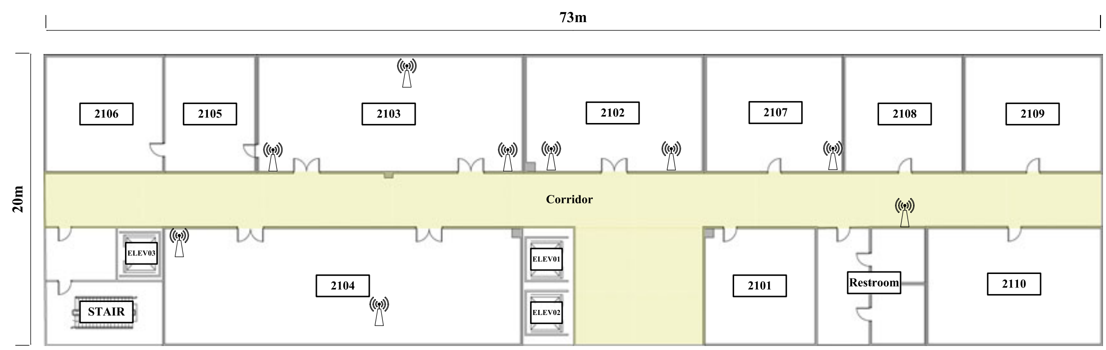

Fig. 4. Layout of the 21st floor in our experimental study.

TABLE II
THE PERCENTAGE STANDARD DEVIATIONS AND CORRELATION COEFFICIENTS OF DIFFERENT KINDS OF FINGERPRINTS

metrics	RSS	SSD	HLF
PSD	14.9%	7.1%	3.6%
correlation coefficient	0.4339	0.6302	0.8276

changing environment, and spatial discrimination. So, the combination of them by using our proposed WiFi-FAGOT can improve the positioning performance to a certain degree.

2) Accuracy: As compared with the existing fusion methods, our proposed WiFi-FAGOT can enhance accuracy well. First, the weights constructed from GFP can fully excavate the intrinsic complementarity among different kinds of fingerprints. The accuracy can be improved by fusing these weights. Second, our proposed OCS algorithm can further improve the accuracy by decreasing the weight selection errors induced by the RSS direct matching. The simulation results show that the performance of our proposed WiFi-FAGOT is much closer to the Cramér-Rao lower bound (CRLB) [36], [37] as compared with other existing methods in the following section. Here, we just discuss fusion of three kinds of fingerprints (features); our method can still improve the accuracy as long as the added features satisfy the principle of ensemble learning [38].

IV. EXPERIMENTAL SETUP AND RESULTS

We compare our proposed WiFi-FAGOT framework with four existing fusion methods: DFC [27], MMSE [29], DFPS [33] and MUCUS [30]. The root mean square error (RMSE) is defined as

$$\mathrm{RMSE} = \sqrt{\frac{1}{J}\sum\nolimits_{n=1}^{J}\left[(\hat{x}_n - x)^2 + (\hat{y}_n - y)^2\right]} \tag{28}$$

where $[\hat{x}_n, \hat{y}_n]^T$ represents the n-th location estimate, and $[x, y]^T$ is the true location of the source, and J is the number of experiment trials.

A. Real Office Scenario

The experiment was carried at the 21st floor of the Innovation building on the campus of University of Electronic Science and Technology of China. The area is about 73 m $\times$ 20 m, i.e., 1460 m^2. It mainly includes 10 offices, one corridor, and 9 APs, which are sparsely deployed to guarantee that at least 3 APs are detectable at each grid point, as shown in Fig. 4. First, we divide the whole area into many grid points and the distance between two adjacent grid points is 0.8 m. We hold an Android smartphone arbitrarily to collect RSS fingerprints. At each grid point, we collect $M = 20$ and $N = 10$ RSS measurements for $\boldsymbol{GF}_1$ and $\boldsymbol{GF}'_1$, respectively. Note that our fusion approach is effective regardless of the selected values of M and N. Specifically, at each grid, we use $\boldsymbol{GF}_1$ and $\boldsymbol{GF}'_1$ to derive another fingerprints, i.e., $\boldsymbol{GF}_2$, $\boldsymbol{GF}'_2$, $\boldsymbol{GF}_3$, and $\boldsymbol{GF}'_3$. Then, we can obtain the WiFi-based GOOF $\boldsymbol{GF}$ and $\boldsymbol{GF}'$. In the online phase, we collect 1200 RSS testing samples at 80 different grid points on the next day. The AP and interior environment are shown in Fig. 5.

As shown in Fig. 6, the RMSEs of DFC and DFPS are 3.55 m and 3.59 m, respectively, close to that of HLF, implying that these two fusion methods cannot fully exploit the complementarity among different kinds of fingerprints. MMSE performs

Fig. 5. The interior environment and AP in our experimental study.

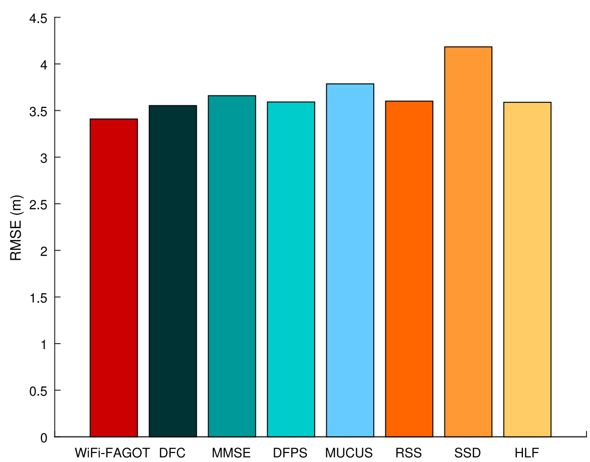

Fig. 6. The RMSEs of different localization methods.

worse than the above two fusion methods because MMSE adopts the GIFP strategy, and thus degrades the performance of localization in this office environment. The worst one is MUCUS whose RMSE is 3.78m because MUCUS does not exploit the offline knowledge, i.e., GFP and OCS, and it needs more online testing samples to yield a more accurate localization result, which is not applicable for WiFi localization because the RSS measurements in WiFi environment need more collecting time than that of the platform used in [30]. Note that the RMSE of our proposed WiFi-FAGOT is 3.4 m, which outperforms other methods.

We also illustrate the cumulative distribution function (CDF) of RMSE of these methods in Fig. 7, which shows that WiFi-FAGOT reduces the 90th percentile RMSE by 13.73%, 14.08%, 22.1%, 25.77%, 21.02%, 31.23%, and 21.33%, as compared with DFC, MMSE, DFPS, MUCUS, RSS, SSD, and HLF, respectively. This improvement comes from the joint utilization of GFP and OCS.

To reveal the impact of the number of different kinds of fingerprints on the localization performance, we compare the RMSEs of WiFi-FAGOT, DFC, MMSE, DFPS and MUCUS with two and three kinds of fingerprints in Fig. 8. Note that the case of two different kinds of fingerprints discussed here

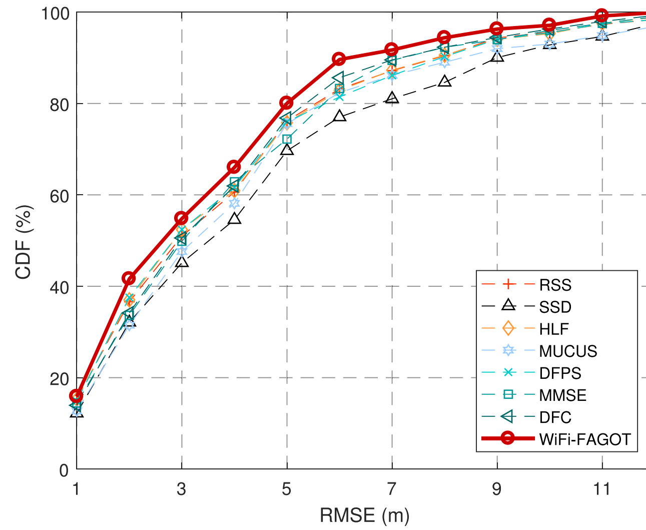

Fig. 7. The CDFs of different localization methods.

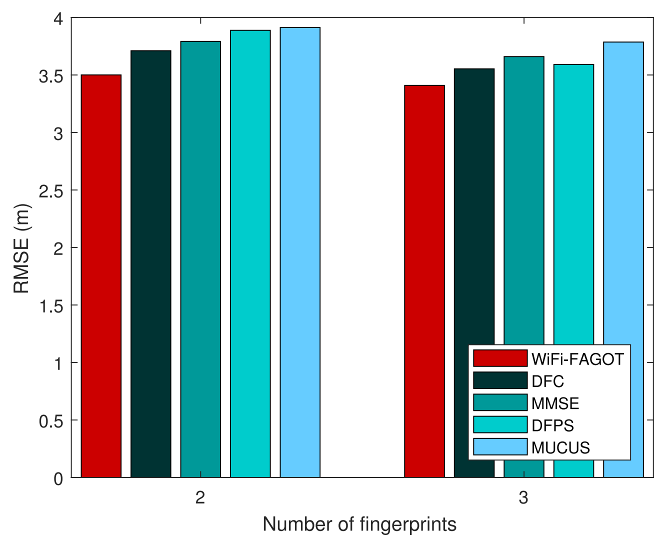

Fig. 8. The RMSEs versus different number of fingerprints.

represents the average RMSE of all combinations of two kinds of fingerprints in $\boldsymbol{GF}$. The WiFi-FAGOT with three kinds of fingerprints performs the best as compared with other cases. For the case of two different kinds of fingerprints, WiFi-FAGOT also performs better than other methods, which also verifies the effectiveness of our method. These results show that our proposed WiFi-FAGOT can fully leverage the complementarity among different kinds of fingerprints, and thus overcomes the drawbacks of other fusion methods.

Next, we evaluate the localization performance of two different grid matching strategies, i.e., RDM and OCS. As shown in Fig. 9, WiFi-FAGOT always outperforms DFC regardless of the matching strategies. Note that RDM chooses the weights by using RDM which is very sensitive to the fluctuation of RSS, while OCS chooses the weights based on the prediction of the optimal classifier obtained in the offline phase. So, OCS has a higher probability of selecting true fusion weights, and thus enhances the performance of localization system significantly. Note that the WiFi-FAGOT with RDM can also outperform

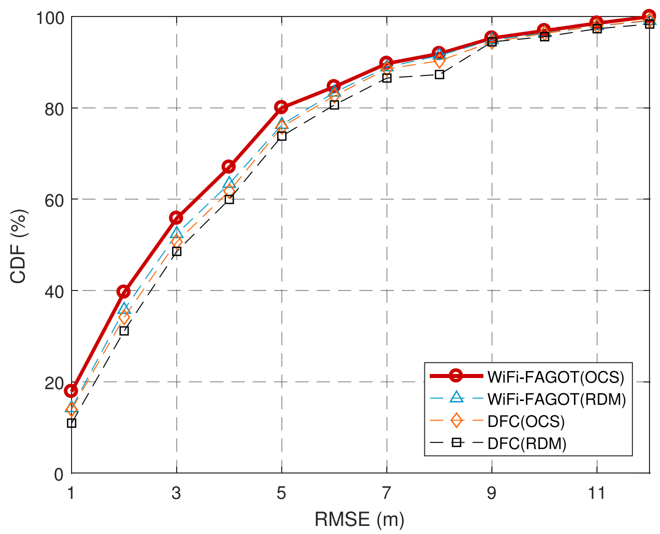

Fig. 9. The CDFs versus different matching strategy.

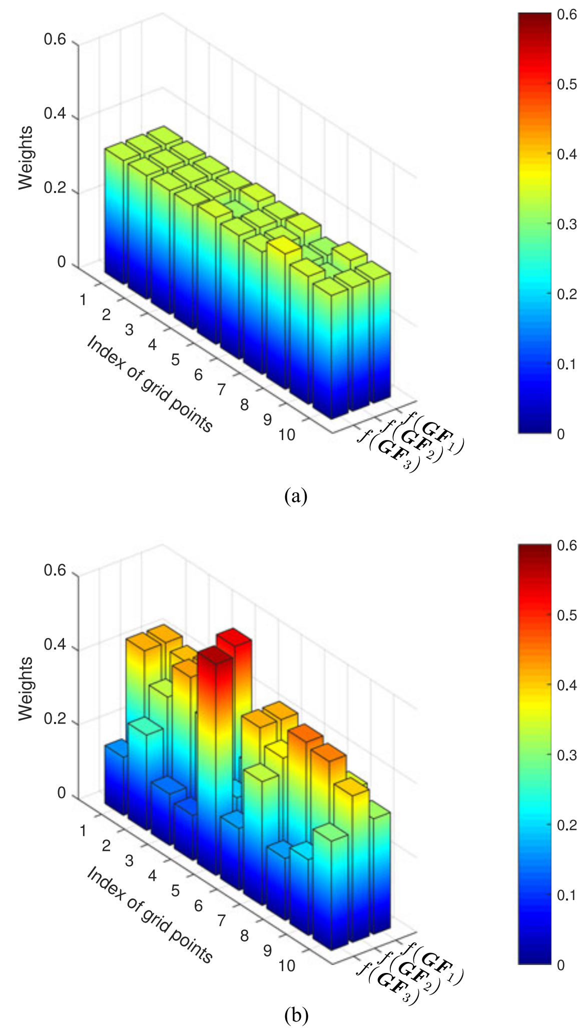

Fig. 10. The comparison of fusion weights of FP and our proposed GFP.

DFC with OCS because the WiFi-FAGOT successfully resorts to the knowledge of GFP, which can fully leverage the intrinsic complementarity among different kinds of fingerprints, and thus obtains the improvement in accuracy significantly.

To clarify the differences between FP and our proposed GFP, we illustrate the weights assignments by FP and GFP in Fig. 10. Owing to the limited space, we only list the weights of 10 grid points for comparison. The weights assigned by GFP, as shown in Fig. 10(b), exhibit greater differences as compared with those by FP. Fig. 10(a) shows that the weights assigned by DFC at most grid points are close to each other, and thus do not reflect the differences in performance among fingerprints. In comparing Fig. 10(a) and (b), we can find that our proposed WiFi-FAGOT framework can fully exploit the complementarity among different kinds of fingerprints.

B. Heterogeneous Devices

To evaluate the impact of heterogeneous devices, we conducted an experiment on the fourth floor of the LiRen Building in the campus of University of Electronic Science and Technology of China. The area is about 11.5 m $\times$ 12 m with 4 detectable APs. We divide the area into many grid points and the distance between two adjacent grid points is 1.2 m.

Specifically, we construct RSS fingerprints with a Vivo smartphone. At each grid point, we collect 60 and 40 RSS measurements for $\boldsymbol{GF}_1$ and $\boldsymbol{GF}'_1$, respectively. In the online phase, we use both Vivo and Huawei smartphones to evaluate the performance of the WiFi-FAGOT framework. At each grid point, we collected 40 RSS testing samples for both devices.

Fig. 11 compares the CDFs of different algorithms versus heterogeneous devices. We can observe that WiFi-FAGOT performs the best in Fig. 11(a) for device 1 (Vivo smartphone), reducing the 90th percentile RMSE by 9.8%, 27.5%, 9.8%, 31.45%, 32.65%, 29.19%, and 27.16%, as compared with DFC, MMSE, DFPS, MUCUS, RSS, SSD, HLF, respectively. Similarly, in Fig. 11(b) for device 2 (Huawei smartphone), it reduces the 90th percentile RMSE by 7.56%, 11.76%, 10.67%, 31.95%, 27.45%, 18.79%, and 29.58%, as compared with DFC, MMSE, DFPS, MUCUS, RSS, SSD, HLF, respectively. The results demonstrate that no matter what devices a user uses in the online phase, our proposed WiFi-FAGOT can make full use of the intrinsic complementarity among different kinds of fingerprints, and thus achieves superior performance over other methods.

C. Changing Environment

Note that the experiments conducted in Sections IV-A and IV-B are typical changing environments because we constructed fingerprints and conducted tests on different days. To better clarify the adaptivity of our proposed WiFi-FAGOT, we construct the WiFi RSS by using the path-loss model [39]

$$P_l = P_0 - 10\gamma \log\left(\frac{d_l}{d_0}\right) + n_l, \tag{29}$$

where P_l in dBm denotes the power received at the target transmitted by the l-th AP, d_l is the distance between the target and the l-th AP. P_0 is the received power in dBm at a reference distance d_0, γ is the path loss factor and n_l is a zero-mean Gaussian distributed random variable with variance σ_l^2.

Assume that four APs are placed at the four corners of a room of size 196 m^2 at positions $[0\,\mathrm{m}, 0\,\mathrm{m}]^T$, $[0\,\mathrm{m}, 14\,\mathrm{m}]^T$, $[14\,\mathrm{m}, 0\,\mathrm{m}]^T$, $[14\,\mathrm{m}, 14\,\mathrm{m}]^T$, respectively. At each grid point, we generated 60 and 40 RSS measurements for $\boldsymbol{GF}_1$ and $\boldsymbol{GF}'_1$, respectively. In the online phase, we generated 100 RSS test-

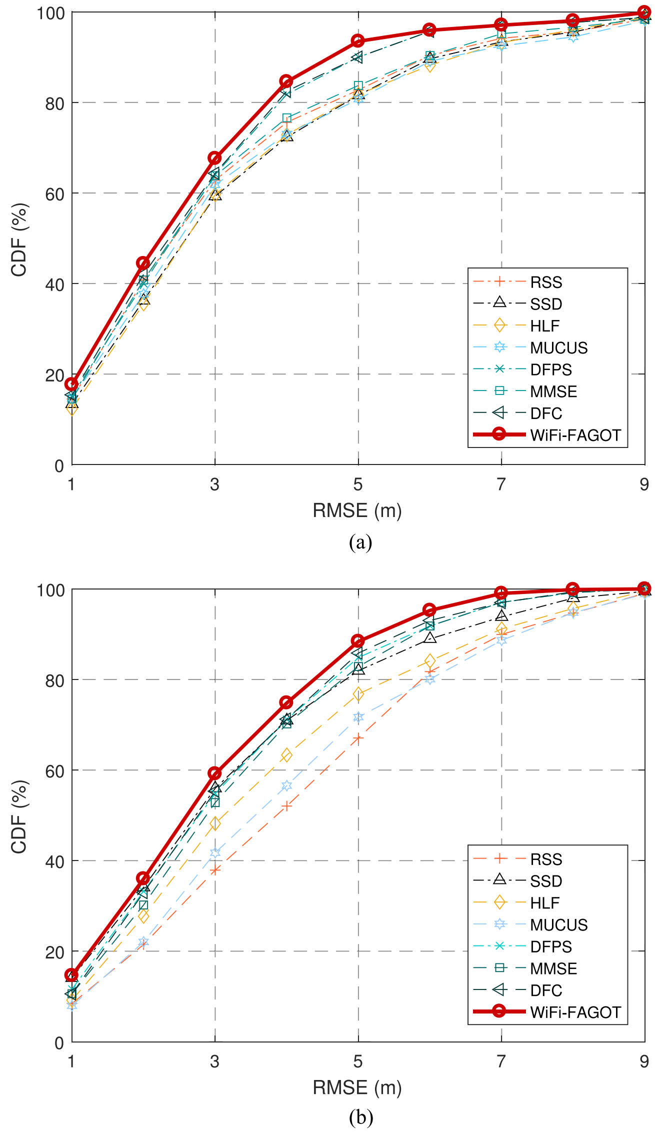

Fig. 11. The CDFs of different algorithms versus heterogeneous devices. (a) Device 1. (b) Device 2.

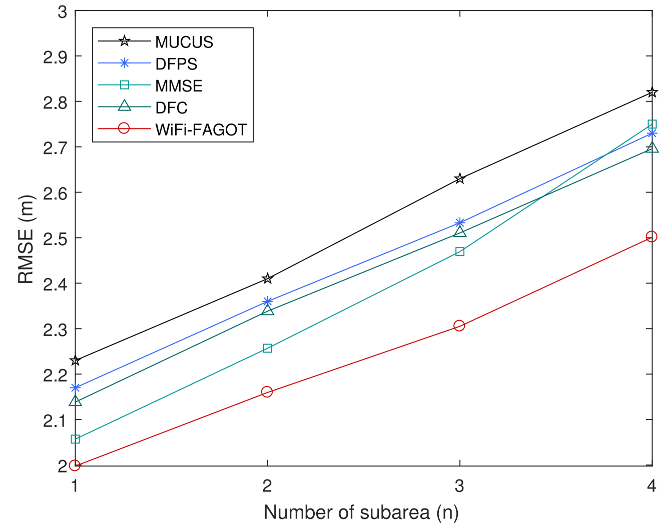

Fig. 12. The RMSEs versus the number of subareas.

TABLE III
THE DIFFERENT PATH LOSS FACTORS USED IN OUR SIMULATION

Path loss factor	The number of subareas			
	$n' = 1$	$n' = 2$	$n' = 3$	$n' = 4$
γ	$\gamma_1 = 2$	$\gamma_1 = 2$ $\gamma_2 = 3$	$\gamma_1 = 2$ $\gamma_2 = 3$ $\gamma_3 = 4$	$\gamma_1 = 2$ $\gamma_2 = 3$ $\gamma_3 = 4$ $\gamma_4 = 5$

ing samples at each grid point. The WiFi-based GOOF is then generated from the above RSS fingerprints.

To elicit the numerical analysis, we partitioned the indoor environment from one to four subareas with different path loss factor γ, as shown in Table III, in which $n' = 1$ means that $\gamma_1 = 2$ in the path-loss model, i.e., the indoor environment does not change; $n' = 2$ means that we use two different path loss factors $\gamma_1 = 2$ and $\gamma_2 = 3$ to simulate the changing indoor environment. The different $\gamma' s$ for $n' = 3$ and $n' = 4$ are also listed in Table III. Fig. 12 depicts the RMSEs versus the number of subareas. Note that the performance of MMSE degrades faster than other algorithms as the complexity of environment increases because MMSE adopts GIFP for fusion. Although DFC is an adaptive one based on GDFP, the FP and matching strategies of DFC degenerate its performance. Thus, the RMSE of DFC increases faster than our approach. DFPS, which combines delta signal strength with RSS directly, does not consider the importance of different kinds of fingerprints, and thus the RMSE also increases faster than our method. MUCUS also degrades quickly as the complexity of the environment increases because it only exploits the predictions of test samples and will lead to cumulative RMSE as most predictions are wrong. Comparatively, the more complex the indoor environment is, the more superior our proposed approach will be. Hence, our WiFi-FAGOT framework is more robust to the changing environment than the other methods.

D. Comparison to the Cramér–Rao Lower Bound (CRLB)

Next, we compare RMSEs of different algorithms with the Cramér-Rao lower bound (CRLB) of RSS-based localization [36], [37] via simulations. CRLB provides the lower bound on the covariance of estimates of an unknown parameter $\hat{\boldsymbol{p}}$. Here, $\hat{\boldsymbol{p}} = [\hat{x}, \hat{y}]^T$ is the estimate of the ground truth location $\boldsymbol{p} = [x, y]^T$ of a gird point. We assume RSS is also generated from (29), and the layout of the environment and APs are the same as described in Section IV-C. For better understanding, we first define the signal-to-noise ratio (SNR) in dB as the mean of squared distance over noise variance. Thus, σ_i^2 can be obtained using $\sigma_i^2 = \frac{d_i^2}{10^{\mathrm{SNR}/10}}$.

We follow the derivation of [36], [37] to calculate the RSS-based CRLB. Denote CRLBs for x and y as $Var(\hat{x})$ and $Var(\hat{y})$, respectively, and the corresponding CRLB for $\boldsymbol{p}$ is

$$Var(\hat{\boldsymbol{p}}) = Var(\hat{x}) + Var(\hat{y}) = \frac{\sum_{i=1}^{L} \frac{\rho_i}{d_i^2}}{\sum_{i=1}^{L} \sum_{j=1, j \neq i}^{L} \rho_i \rho_j C_{ij}}, \tag{30}$$

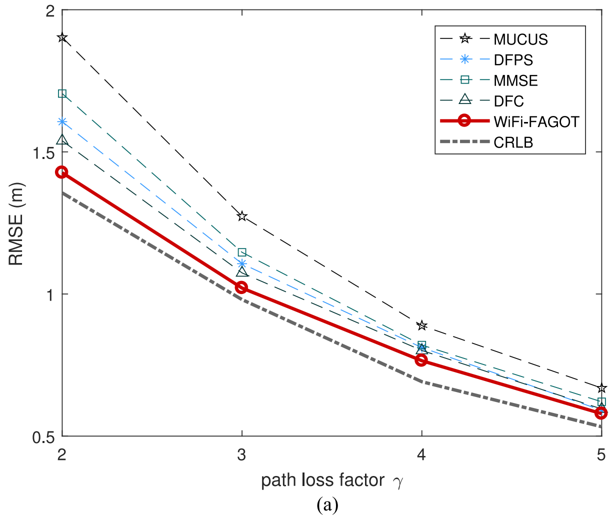

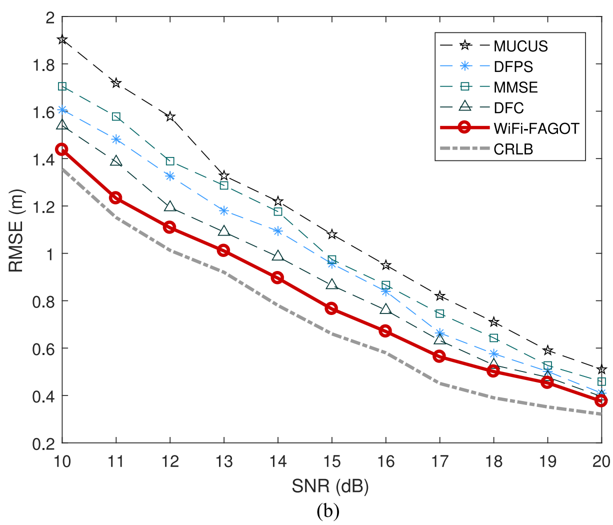

Fig. 13. The RMSE of different methods compared with CRLB. (a) Path loss factor γ. (b) SNR (dB).

where L is the number of APs, $C_{ij} = (\frac{\cos\varphi_i \sin\varphi_j}{d_i d_j} - \frac{\cos\varphi_j \sin\varphi_i}{d_j d_i})^2$, $\sin\varphi_i = \frac{y-y_i}{d_i}$, $\cos\varphi_i = \frac{x-x_i}{d_i}$ and $\rho_i = (\frac{10\gamma}{\sigma_i \log 10})^2$. Note that $Var(\hat{\boldsymbol{p}})$ represents the mean square error (MSE), and in this work we use $\sqrt{Var(\hat{\boldsymbol{p}})}$ to serve as a benchmark to compare with the RMSEs of different methods as shown in Fig. 13. Since we can calculate a CRLB at each grid point, we take their average as the final CRLB. Fig. 13 shows the RMSEs of different methods versus path loss factor γ and SNR. We can observe that the RMSEs of WiFi-FAGOT is much closer to the CRLB than other methods, thus validating the superiority of our proposed WiFi-FAGOT.

V. Conclusion

In this paper, we have proposed an accurate WiFi localization approach by Fusing A Group Of fingerprinTs (WiFi-FAGOT) via GFP. WiFi-FAGOT first constructs a WiFi-based GOOF in the offline phase, which consists of RSS, SSD, and HLF. Then, instead of direct localization by using the WiFi-based GOOF, we design multiple classifiers by training each fingerprint in the WiFi-based GOOF, namely, GOOF-classifiers. To overcome the drawbacks of existing fusion localization methods, we have also proposed a GFP construction algorithm to fully exploit the complementarity among different kinds of fingerprints. GFP outperforms the conventional FP in localization accuracy. In the online phase, we have derived the OCS algorithm to intelligently choose a fusion profile in GFP for higher localization. Although WiFi-FAGOT is also based on the RSS fingerprint, it can improve the accuracy of localization by fully leveraging all fingerprints without modifying any hardware, and is thus very promising for indoor localization in the WiFi environment.

References

[1] X. Sun and N. Ansari, "EdgeIoT: Mobile edge computing for the internet of things," *IEEE Commun. Mag.*, vol. 54, no. 12, pp. 22–29, Dec. 2016.

[2] X. Liu and N. Ansari, "Green relay assisted D2D communications with dual batteries in heterogeneous cellular networks for IoT," *IEEE Internet Things J.*, vol. 4, no. 5, pp. 1707–1715, Oct. 2017.

[3] T. Wigren, "Adaptive enhanced cell-ID fingerprinting localization by clustering of precise position measurements," *IEEE Trans. Veh. Technol.*, vol. 56, no. 5, pp. 3199–3209, Sep. 2007.

[4] G. Wang, Y. Li, and N. Ansari, "A semidefinite relaxation method for source localization using TDOA and FDOA measurements," *IEEE Trans. Veh. Technol.*, vol. 62, no. 2, pp. 853–862, Feb. 2013.

[5] J. Talvitie, M. Renfors, and E. S. Lohan, "Distance-based interpolation and extrapolation methods for RSS-based localization with indoor wireless signals," *IEEE Trans. Veh. Technol.*, vol. 64, no. 4, pp. 1340–1353, Apr. 2015.

[6] G. Wang, S. Cai, Y. Li, and N. Ansari, "A bias-reduced nonlinear WLS method for TDOA/FDOA-based source localization," *IEEE Trans. Veh. Technol.*, vol. 65, no. 10, pp. 8603–8615, Oct. 2016.

[7] L. Chen, K. Yang, and X. Wang, "Robust cooperative Wi-Fi fingerprint-based indoor localization," *IEEE Internet Things J.*, vol. 3, no. 6, pp. 1406–1417, Dec. 2016.

[8] S. S. Chawathe, "Low-latency indoor localization using bluetooth beacons," in *Proc. 12th Int. IEEE Conf. Intell. Transport. Syst.*, 2009, pp. 1–7.

[9] Y.-T. Chen, C.-L. Yang, Y.-K. Chang, and C.-P. Chu, "A RSSI-based algorithm for indoor localization using ZigBee in wireless sensor network," in *Proc. 15th Int. Conf. Distrib. Multimedia Syst.*, 2009, pp. 70–75.

[10] S. Amendola, R. Lodato, S. Manzari, and C. Occhiuzzi, "RFID technology for IoT-based personal healthcare in smart spaces," *IEEE Internet Things J.*, vol. 1, no. 2, pp. 144–152, Apr. 2014.

[11] X. Guo, L. Chu, and X. Sun, "Accurate localization of multiple sources using semidefinite programming based on incomplete range matrix," *IEEE Sens. J.*, vol. 16, no. 13, pp. 5319–5324, Jul. 2016.

[12] N. Patwari, J. N. Ash, S. Kyperountas, A. O. Hero, R. L. Moses, and N. S. Correal, "Locating the nodes: Cooperative localization in wireless sensor networks," *IEEE Signal Process. Mag.*, vol. 22, no. 4, pp. 54–69, Jul. 2005.

[13] M. Z. Win *et al.*, "Network localization and navigation via cooperation," *IEEE Commun. Mag.*, vol. 49, no. 5, pp. 56–62, May 2011.

[14] Y. Shen, S. Mazuelas, and M. Z. Win, "Network navigation: Theory and interpretation," *IEEE J. Sel. Areas Commun.*, vol. 30, no. 9, pp. 1823–1834, Oct. 2012.

[15] S. Mazuelas *et al.*, "Robust indoor positioning provided by real-time RSSI values in unmodified WLAN networks," *IEEE J. Sel. Topics Signal Process.*, vol. 3, no. 5, pp. 821–831, Oct. 2009.

[16] J. Yang and Y. Chen, "Indoor localization using improved RSS-based lateration methods," in *Proc. IEEE GLOBECOM*, 2009, pp. 1–6.

[17] S. Mazuelas *et al.*, "Topology assessment provided by weighted barycentric parameters in harsh environment wireless location systems," *IEEE Trans. Signal Process.*, vol. 58, no. 7, pp. 3842–3857, Jul. 2010.

[18] M. Kotaru, K. Joshi, D. Bharadia, and S. Katti, "SpotFi: Decimeter level localization using WiFi," *ACM SIGCOMM Comput. Commun. Rev.*, vol. 45, no. 4, pp. 269–282, 2015.

[19] M. Brunato and R. Battiti, "Statistical learning theory for location fingerprinting in wireless LANs," *Comput. Netw.*, vol. 47, no. 6, pp. 825–845, 2005.

[20] Z. Yang, C. Wu, and Y. Liu, "Locating in fingerprint space: Wireless indoor localization with little human intervention," in *Proc. 18th Annu. Int. Conf. Mobile Comput. Netw.*, 2012, pp. 269–280.

[21] A. K. M. M. Hossain, H. N. Van, Y. Jin, and W. S. Soh, "Indoor localization using multiple wireless technologies," in *Proc. IEEE Int. Conf. Mobile Adhoc Sens. Syst.*, 2008, pp. 1–8.

[22] M. B. Kjrgaard and C. V. Munk, "Hyperbolic location fingerprinting: A calibration-free solution for handling differences in signal strength (concise contribution)," in *Proc. IEEE 6th Annu. IEEE Int. Conf. Pervasive Comput. Commun.*, 2008, pp. 110–116.

[23] T. Roos, P. Myllymki, H. Tirri, P. Misikangas, and J. Sievnen, "A probabilistic approach to WLAN user location estimation," *Int. J. Wireless Inf. Netw.*, vol. 9, no. 3, pp. 155–164, 2002.

[24] S. H. Fang, T. N. Lin, and K. C. Lee, "A novel algorithm for multipath fingerprinting in indoor WLAN environments," *IEEE Trans. Wireless Commun.*, vol. 7, no. 9, pp. 3579–3588, Sep. 2008.

[25] Z. L. Wu, C. H. Li, K. Y. Ng, and K. R. P. H. Leung, "Location estimation via support vector regression," *IEEE Trans. Mobile Comput.*, vol. 6, no. 3, pp. 311–321, Mar. 2007.

[26] H. Zou, X. Lu, H. Jiang, and L. Xie, "A fast and precise indoor localization algorithm based on an online sequential extreme learning machine," *Sensors*, vol. 15, no. 1, pp. 1804–1824, 2015.

[27] S. H. Fang, Y. T. Hsu, and W. H. Kuo, "Dynamic fingerprinting combination for improved mobile localization," *IEEE Trans. Wireless Commun.*, vol. 10, no. 12, pp. 4018–4022, Dec. 2011.

[28] S. H. Fang, C. H. Wang, T. Y. Huang, C. H. Yang, and Y. S. Chen, "An enhanced ZigBee indoor positioning system with an ensemble approach," *IEEE Commun. Lett.*, vol. 16, no. 4, pp. 564–567, Apr. 2012.

[29] Y. Gwon, R. Jain, and T. Kawahara, "Robust indoor location estimation of stationary and mobile users," in *Proc. IEEE INFOCOM*, 2004, pp. 1032–1043.

[30] X. Guo and N. Ansari, "Localization by fusing a group of fingerprints via multiple antennas in indoor environment," *IEEE Trans. Veh. Technol.*, vol. 66, no. 11, pp. 9904–9915, Nov. 2017.

[31] F. Gu, J. Niu, and L. Duan, "WAIPO: A fusion-based collaborative indoor localization system on smartphones," *IEEE/ACM Trans. Netw.*, vol. 25, no. 4, pp. 2267–2280, Aug. 2017.

[32] A. K. M. M. Hossain, Y. Jin, W. S. Soh, and H. N. Van, "SSD: A robust RF location fingerprint addressing mobile devices' heterogeneity," *IEEE Trans. Mobile Comput.*, vol. 12, no. 1, pp. 65–77, Jan. 2013.

[33] S. H. Fang and C. H. Wang, "A novel fused positioning feature for handling heterogeneous hardware problem," *IEEE Trans. Commun.*, vol. 63, no. 7, pp. 2713–2723, Jul. 2015.

[34] S. H. Fang and T. N. Lin, "Cooperative multi-radio localization in heterogeneous wireless networks," *IEEE Trans. Wireless Commun.*, vol. 9, no. 5, pp. 1547–1551, May 2010.

[35] H. Liu, H. Darabi, P. Banerjee, and J. Liu, "Survey of wireless indoor positioning techniques and systems," *IEEE Trans. Syst., Man, Cybern. C, Appl. Rev.*, vol. 37, no. 6, pp. 1067–1080, Nov. 2007.

[36] N. Patwari and A. O. Hero, "Location estimation accuracy in wireless sensor networks," in *Proc. IEEE 36th Asilomar Conf. Signals, Syst. Comput.*, 2002, vol. 2, pp. 1523–1527.

[37] X. Zheng, H. Liu, J. Yang, Y. Chen, R. P. Martin, and X. Li, "A study of localization accuracy using multiple frequencies and powers," *IEEE Trans. Parallel Distrib. Syst.*, vol. 25, no. 8, pp. 1955–1965, Aug. 2014.

[38] Z. Zhang, H. Liu, B. Fu, and Z. Wu, "Generalized ambiguity decompositions for classification with applications in active learning and unsupervised ensemble pruning," in *Proc. 31st AAAI Conf. Artif. Intell.*, 2017, pp. 2073–2079.

[39] R. Zekavat and R. Buehrer, *Handbook of Position Location: Theory, Practice, and Advances*. New York, NY, USA: Wiley, 2011.

Xiansheng Guo (S'07–M'11) received the B.Eng. degree from Anhui Normal University, Wuhu, China, in 2002, the M.Eng. degree from the Southwest University of Science and Technology, Mianyang, China, in 2005, and the Ph.D. degree from the University of Electronic Science and Technology of China (UESTC), Chengdu, China, in 2008. From 2008 to 2009, he was a Research Associate with the Department of Electrical and Electronic Engineering, University of Hong Kong. From 2012 to 2014, he was a Research Fellow with the Department of Electronic Engineering, Tsinghua University. He is currently an Associate Professor with the Department of Electronic Engineering, UESTC. He was a Research Scholar with the Advanced Networking Laboratory, Department of Electrical and Computer Engineering, New Jersey Institute of Technology, Newark, NJ, USA, from 2016 to 2017. His research interests include array signal processing, wireless localization, machine learning, information fusion, and software radio design.

Lin Li (S'12) received the B.Eng. degree from the University of Electronic Science and Technology of China, Chengdu, China, in 2016, where he is currently working toward the Master's degree in the Department of Electronic Engineering. His research interests include indoor localization, machine learning, ensemble learning, and information fusion.

Nirwan Ansari (S'78–M'83–SM'94–F'09) received the B.S.E.E. (*summa cum laude* with a perfect GPA) degree from the New Jersey Institute of Technology (NJIT), Newark, NJ, USA, the M.S.E.E. degree from the University of Michigan, Ann Arbor, MI, USA, and the Ph.D. degree from Purdue University, West Lafayette, IN, USA. He is currently a Distinguished Professor with the Department of Electrical and Computer Engineering, NJIT. He has also been a Visiting (Chair) Professor at several universities. He authored a book entitled *Green Mobile Networks: A Networking Perspective* (New York, NY, USA: Wiley–IEEE Press, 2017) with T. Han, and coauthored two other books. He has also (co)authored more than 500 technical publications, with more than 250 published in widely cited journals/magazines. He has guest-edited a number of special issues covering various emerging topics in communications and networking. He has served on the Editorial/Advisory Board of more than ten journals. He has also been granted 36 U.S. patents. His current research interests include green communications and networking, cloud computing, and various aspects of broadband networks. He was a member-at-large of the IEEE Communications Society (COMSOC) Board of Governors, has chaired COMSOC technical committees and the HPSR Steering Committee, has served in various committees such as the IEEE Fellow Committee, and has been actively organizing numerous IEEE International conferences/symposia/workshops. He has frequently been delivering keynote addresses, distinguished lectures, tutorials, and invited talks. Some of his recognitions include several Excellence in Teaching Awards, several Best Paper Awards, the NCE Excellence in Research Award, the IEEE TC-CSR Distinguished Technical Achievement Award, TCGCC Distinguished Technical Achievement Recognition Award, the COMSOC AHSN TC Technical Recognition Award, the NJ Inventors Hall of Fame Inventor of the Year Award, the Thomas Alva Edison Patent Award, the Purdue University Outstanding Electrical and Computer Engineer Award, and designation as a COMSOC Distinguished Lecturer.

Bin Liao (S'09–M'13–SM'16) received the B.Eng. and M.Eng. degrees from Xidian University, Xi'an, China, in 2006 and 2009, respectively, and the Ph.D. degree from the University of Hong Kong, Hong Kong, in 2013. From September 2013 to January 2014, he was a Research Assistant with the Department of Electrical and Electronic Engineering, The University of Hong Kong. From August 2016 to October 2016, he was a Research Scientist with the Department of Electrical and Electronic Engineering, The University of Hong Kong. He is currently an Associate Professor with the College of Information Engineering, Shenzhen University, Shenzhen, China. His research interests include sensor array processing, adaptive filtering, and convex optimization, with applications to radar, navigation, and communications. He received the 2016 IEEE DSP Best Paper Award and 2017 IEEE DSP Best Paper Award. He is an Associate Editor for *IET Signal Processing*, the IEEE ACCESS, and *Multidimensional Systems and Signal Processing*.